Aeolian Research 8 (2013) 85–100

Contents lists available at SciVerse ScienceDirect

Aeolian Research

journal homepage: www.elsevier.com/locate/aeolia

Thin, pedoturbated, and locally sourced loess in the western Upper Peninsula of Michigan

Michael D. Luehmann *, Randall J. Schaetzl, Bradley A. Miller, Michael E. Bigsby

Department of Geography, Michigan State University, Geography Building, 673 Auditorium Rd., Room 1B, East Lansing, MI 48824-1117, United States

ARTICLE INFO

Article history:
Received 12 May 2012
Revised 21 November 2012
Accepted 21 November 2012
Available online 1 February 2013

Keywords:
Loess
Michigan
Particle size filtering
Bimodal texture curves
Pedoturbation

ABSTRACT

Soil surveys document thin but discontinuous loess deposits across large tracts of Michigan's western Upper Peninsula (UP), which we informally call the Peshekee loess. Our study is the first to examine the distribution, thickness and textural characteristics of these loess deposits, and speculate as to their origins. Peshekee loess is typically 20–70 cm thick and underlain by sandy glacial deposits. At most sites, pedoturbation has mixed some of the lower materials into the loess, resulting in a particle size mode within the 25–75 μm fraction (from the loess), but also a secondary mode in the 250–500 μm fraction (from the pedoturbated sand). We introduce a method by which the mixed sand data are removed, or "filtered out," of the original particle size data, to better reflect the original textural characteristics of the loess. Our data – from 237 upland sites – show that the textural and thickness attributes of the loess change markedly across the region, pointing to the influence of many localized loess sources, and suggesting that this loess was transported mainly over short distances. The Peshekee loess deposits were mainly derived locally from moraines, outwash plains, and floodplains of small meltwater streams – interspersed within the region and at its periphery. We identify and name four main loess "core" regions, each of which has distinct characteristics that set it apart, and describe each of these as a unique "type" of loess with one or more local source areas. Loess from each core area overlaps with neighboring loess deposits.

1. Introduction

Loess is found across China, Central Asia, Europe, New Zealand, South America, Alaska, and on both the Great Plains and Central Lowlands of North America, particularly in and near the Mississippi Valley (Smalley, 1975; Follmer, 1996; Mason et al., 1999; Bettis et al., 2003; Roberts et al., 2003) (Fig. 1). Many – although certainly not all – North American loess deposits are associated with glacial episodes, thereby providing a record of environmental change during and after the last glacial phase (Muhs and Bettis, 2003). Interpretation of this record of environmental change requires accurately linking loess stratigraphic sequences to their source areas, along with understanding the spatial characteristics of the loess itself (Mason et al., 1999; Muhs et al., 1999, 2008; Sun, 2002; Schaetzl and Hook, 2008; Aleinikoff et al., 2008; Stanley and Schaetzl, 2011).

In the Midwestern United States, loess can exceed tens of meters in thickness, especially near major meltwater valleys (e.g., Smith, 1942; Olson and Ruhe, 1979; Fehrenbacher et al., 1986; Roberts et al., 2003). The loess deposits generally become thinner away from these valleys, until, at the margins, these deposits become discontinuous and where present, thin and variously mixed into the underlying sediment (Stanley and Schaetzl, 2011; Scull and Schaetzl, 2011; Schaetzl and Luehmann, 2013). Justifiably, the majority of traditional loess research has focused on the thick loess deposits near large river valleys (Smith, 1942; Wascher et al., 1947; Frazee et al., 1970; Olson and Ruhe, 1979; Fehrenbacher et al., 1986; Leigh, 1994; Pye, 1995; Rutledge et al., 1996; Bettis et al., 2003). The relatively thin and discontinuous loess deposits that blanket much of the Great Lakes region have been, until very recently, inadequately mapped and largely unstudied.

On a small-scale map that is sometimes referred to as the "first best loess map" of the USA, Thorp and Smith (1952) identified major loess deposits near the large meltwater valleys in the Midwest, but failed to show some of the smaller, thinner and disjunct deposits farther from them. One such loess deposit that they did identify extends as a narrow finger from northeastern Wisconsin into Iron County, MI (Fig. 1). Later, between 1980 and 2007, independent work performed by Natural Resource Conservation Service (NRCS) personnel, as part of their county-level soil survey operations, confirmed this loess but also identified loess of considerably wider extent in the western Upper Peninsula (UP) (Berndt, 1988; Linsemier, 1997; Schwenner, 2007) (Fig. 2). Many soil series here were defined as having been formed in loess or in a "modified eolian

* Corresponding author. Tel.: +1 586 291 9063; fax: +1 517 432 1671.
E-mail address: luehmann@msu.edu (M.D. Luehmann).

1875-9637/$ - see front matter © 2012 Elsevier B.V. All rights reserved.
http://dx.doi.org/10.1016/j.aeolia.2012.11.003

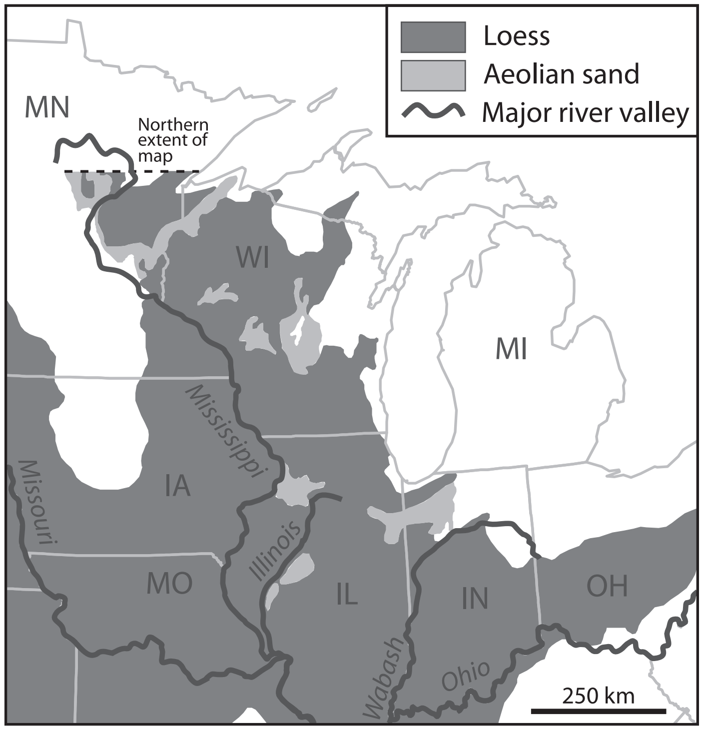

Fig. 1. Extent of loess and aeolian sand deposits in the Midwestern USA, redrawn from Thorp and Smith (1952).

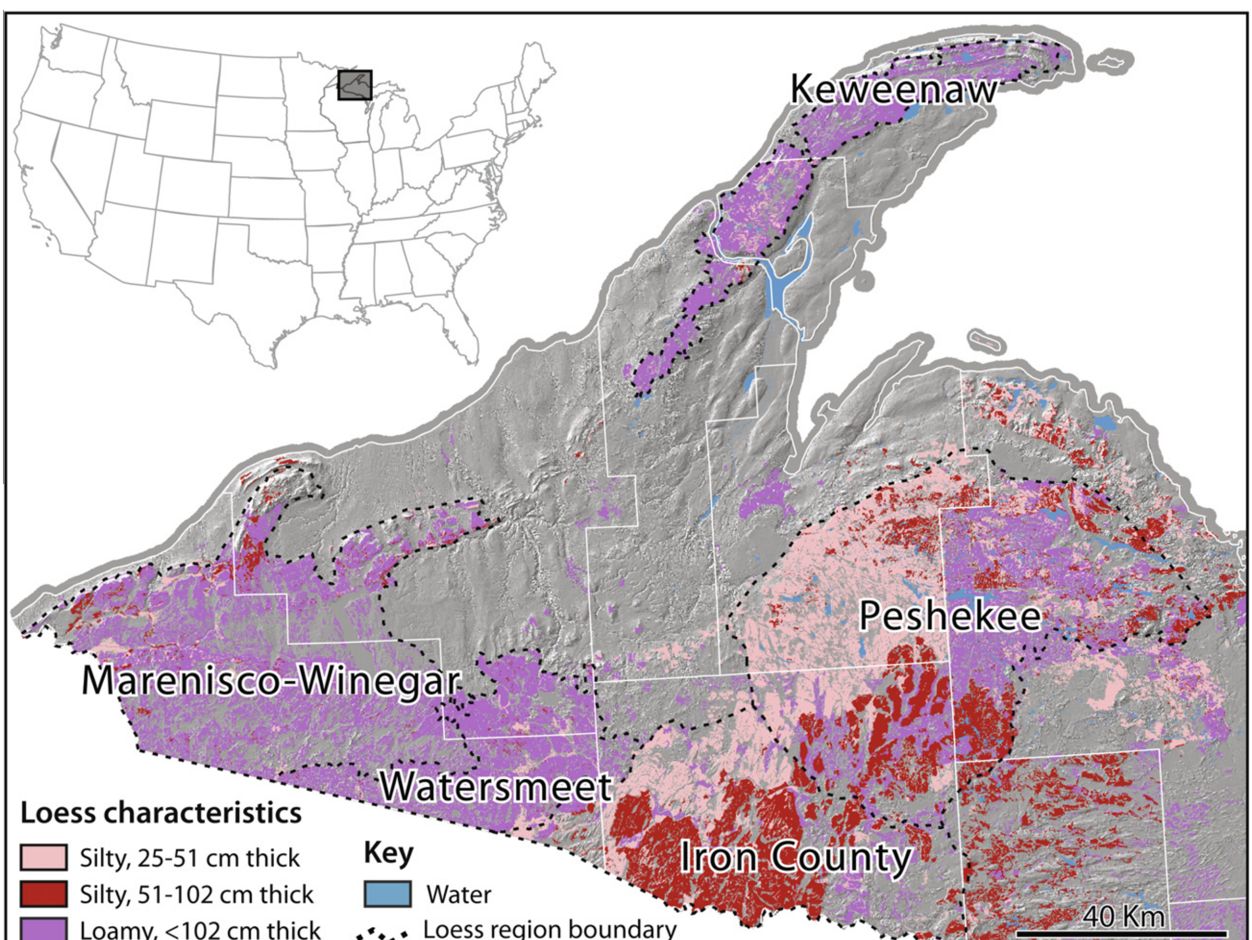

Fig. 2. Loess regions identified within the western Upper Peninsula of Michigan, as indicated on NRCS soil survey maps and as interpreted from Scull and Schaetzl (2011).

Table 1
The most extensive, upland, soil series within five loess regions of the western Upper Peninsula that have some type of silty mantle.

Soil series	NRCS parent material description (upper parent material – lower parent material)	Range of aeolian mantle thickness (cm) (based on NRCS Official Soil Series Description)	Texture class of loess or aeolian mantle (NRCS)	Extent within the loess region (%)
Keweenaw region – fine sandy loess				
Trimountain	Loamy aeolian mantle – gravelly loamy or sandy glacial till	30–69	Fine sandy loam	30.71
Montreal	Loamy aeolian deposits – loamy or sandy till	Not reported	Fine sandy loam	27.23
Other loessal soil series: Michigamme (extent within the loess region, 0.59%)				
Marenisco-Winegar region – sandy loess				
Gogebic	Modified loamy aeolian deposits – loamy and sandy glacial till	53–64	Sandy loam	38.62
Wakefield	Modified loamy aeolian deposits – loamy glacial till	30–46	Silt loam	1.98
Other loessal soil series: Schweitzer, Stutts, Michigamme, and Karlin (extent within the loess region, 3.72%)				
Watersmeet region – sandy/loamy fine sandy loess				
Gogebic	Loamy aeolian deposits – loamy and sandy glacial till	53–64	Sandy loam	35.91
Karlin	Sandy deposits	Not reported	Loamy fine sand	27.03
Other loessal soil series: Pence, Stutts, Michigamme, and Schweitzer (extent within the loess region, 3.34%)				
Iron County region – silt loam loess				
Wabeno	Loess – loamy and sandy till or glacial mud-flow sediment	30–91	Silt loam	23.96
Champion	Modified loamy aeolian material – gravelly sandy or loamy glacial till	41–61	Silt loam/fine sandy loam	9.85
Other loessal soil series: Pence, Karlin, Peavy, Soperton, Gogebic, Sundog, Petticoat, and Pemene (extent within the loess region, 21.96%)				
Peshekee region – silt loam/fine sandy loam loess				
Champion	Modified loamy aeolian material – gravelly sandy oar loamy glacial till	41–61	Silt loam/fine sandy loam	16.35
Keewaydin	Loamy and silty aeolian deposits – till	38–76	Fine sandy loam	9.34
Other loessal soil series: Sundog, Michigamme, Goodman, Petticoat, Amasa, Wabeno, Pence, and Peshekee (extent within the loess region, 25.34%)				

material," often overlying other sediment or bedrock (Table 1). To be fair, we observe that the thickest parts of the loess, as mapped by NRCS personnel, occur in the area initially mapped by Thorp and Smith (1952) (Fig. 1). But to the east and north, new data from the NRCS documented soils – especially on uplands – that had also formed in loess, albeit here the loess was thinner and more discontinuous.

In summary, NRCS data suggest that loess exists in the western UP, but in an area situated far from the major valleys that have long been assumed to have been the major loess sources in the Great Lakes region. There is ample reason to believe that the NRCS data are accurate (Scull and Schaetzl, 2011; Stanley and Schaetzl, 2011). In this study, we explore whether loess actually exists in the western UP – our study area – and attempt to map its distribution, thickness and textural characteristics. To date, no dedicated research has been conducted on these deposits, to determine if this silty mantle is, indeed, loess, or to ascertain its variability.

Because the presumed loess in the study area lies far from the major meltwater valleys, it likely has been derived from other sources. Indeed, loess deposits in central and eastern Wisconsin, and Michigan, have recently been linked to non-traditional loess source areas, such as outwash plains, moraines, glaciolacustrine plains, and mid-size meltwater valleys (Schaetzl, 2008, 2012; Schaetzl and Hook, 2008; Schaetzl and Loope, 2008; Stanley and Schaetzl, 2011; Scull and Schaetzl, 2011). Determination of the sources for these smaller, "interior" loess deposits remains an area of debate (Schaetzl, 2012; Jacobs et al., 2012). Our research is intended to add substance to this debate and to help resolve some of the questions about loess and its source areas, where they occur at the margins of a larger loess region.

The purpose of this study is to determine the spatial characteristics of the (presumed) loess that has been mapped in Baraga, Iron, and Marquette Counties, Michigan – at the northeastern-most extent of the widespread loess deposits in the Midwestern USA. In doing so, we hope to document the importance of short-distance loess transport on recently deglaciated landscapes. Lastly, we introduce a new particle-size data filtering method for studying thin loess deposits like these, and in so doing, emphasize the importance of using this type of "filtered" data for the analysis of sediment with mixed sedimentologic histories.

2. Study area

Using NRCS data, Scull and Schaetzl (2011) identified and named (at small-scale) multiple loess "sheets" throughout Wisconsin and Michigan's western UP. In the western UP they identified, from east to west, the Peshekee, Iron County, Marenisco-Winegar, and Keweenaw loess sheets (Fig. 2). Using NRCS county level soil survey data, similar to Scull and Schaetzl's (2011) approach, we outlined in more detail five loess regions within the western UP (Fig. 2). To do so, first we determined the parent materials(s) for the soil series in the region from the official series descriptions at http://soils.usda.gov/technical/classification/osd/. Table 1 highlights the dominant soil series that comprise each loess region. Textural variations among these loess regions can sometimes be linked to their unique loess sources, although more research must be done in order to accurately determine the loess provenance of each region shown in Fig. 2.

The focus of this research is the Peshekee loess region (Fig. 2), located within the Superior Upland physiographic province (Fenneman, 1938). The landscape, underlain by Precambrian crystalline bedrock (Card, 1990), is extremely heterogeneous, with high (>100 m) local relief in some areas. Final retreat of the Laurentide Ice Sheet (LIS) occurred here ≈11,500 cal. yrs BP (Fig. 3; Hughes and Merry, 1978; Lowell et al., 1999; Pregitzer et al., 2000). Outwash plains, end moraines, ground moraines, and midsize glacial meltwater valleys, all formed at this time, are common on this landscape. Glacial diamict is relatively thin (<30 m) and patchy in most areas – and absent on many bedrock uplands.

The vegetation of this region varies, based on soils, elevation and landscape position (Barrett et al., 1995; Comer et al., 1995; Al-

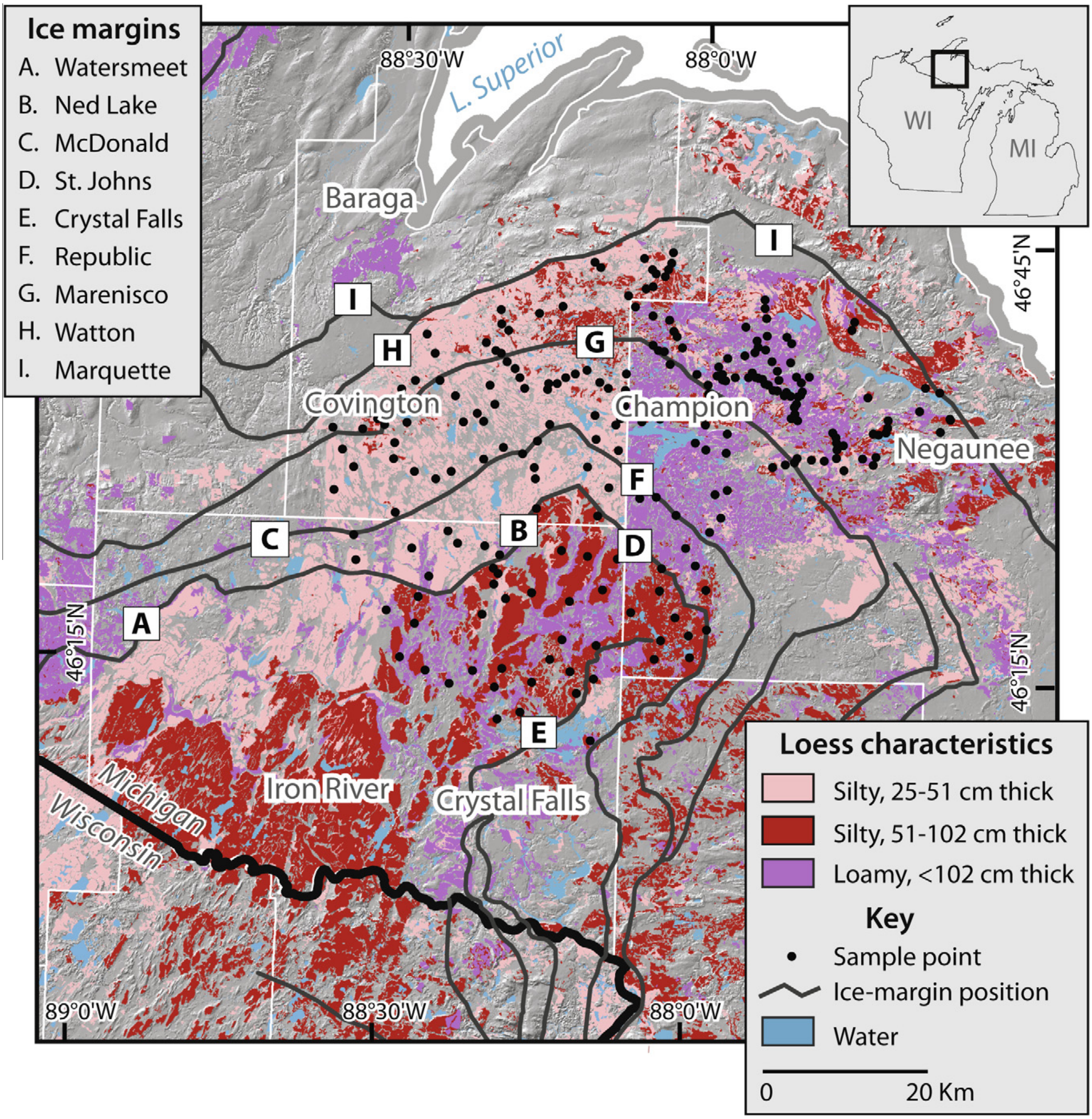

Fig. 3. Ice marginal positions within the western Upper Peninsula, and the locations of the 237 loess samples sampled for this study. Major cities within the study area are also noted.

bert, 1995; Albert and Comer, 2008). Upland sites are dominated by sugar maple (*Acer saccharum*), aspen (*Populus* spp.), red maple (*Acer rubrum*), and American beech (*Fagus grandifolia*), with admixtures of some coniferous tree species. Lowlands generally contain mixed conifer swamp species such as black spruce (*Picea mariana*), northern white cedar (*Thuja occidentalis*), and balsam fir (*Abies balsamea*).

Upland soils within the Peshekee loess region mainly consist of well and moderately well drained Spodosols and Inceptisols. Most of these soils have formed in a silty mantle of differing thicknesses, overlying loamy and sandy sediments, and sometimes resting directly on bedrock (Berndt, 1988; Linsemier, 1997; Schwenner, 2007). Valleys and depressions are commonly occupied by organic rich, poorly drained sands, or by very poorly drained Histosols. As interpreted by the NRCS, the seven dominant loessal soil series mapped within the study area (Berndt, 1988; Linsemier, 1997; Schwenner, 2007) all have formed in fine-textured loess and the underlying loamy and sandy glacial till (Table 2). The main differences among them are in their subsurface diagnostic horizons, i.e., a fragipan and/or argillic horizon, upper solum textures, and loess thicknesses.

3. Methods

3.1. Field methods

Potential loess sample locations, identified and coded in a geographic information system (GIS), all met the following criteria: (1)

Table 2
Dominant soil series within the Peshekee loess region.

Soil series	Taxonomic class	Surface texture	Depth to LD[a] (cm)	Texture below LD[a]	Subsurface diagnostic horizon	Extent within the Peshekee loess region (%)
Champion	Oxyaquic Fragiorthods	Cobbly silt loam	56	Gravelly sandy loam	Spodic Fragipan	11.90
Keewaydin	Typic Haplorthods	Cobbly fine sandy loam	51	Gravelly loamy sand	Spodic	6.00
Michigamme	Fragic Haplorthods	Cobbly silt loam	53	Gravelly fine sand	Spodic Fragipan	3.81
Petticoat	Alfic Haplorthods	Cobbly silt Loam	97	Very gravelly loamy sand	Spodic Argillic	2.65
Goodman	Alfic Haplorthods	Silt loam	64	Sand loam	Spodic Argillic	2.51
Wabeno	Oxyaquic Fragiorthods	Silt loam	61	Gravelly sandy loam	Spodic Fragipan Argillic	2.10
Dishno	Oxyaquic Haplorthods	Cobbly silt loam	46	Very stony loamy sand	Spodic	1.48

[a] LD, lithologic discontinuity.

mapped within one of the series listed in Table 2, (2) located on a broad, flat upland, and (3) presently wooded, thereby negating major disturbances due to cultivation. Sites that met criteria 1–3 were then inspected to determine if they had a silty (or very fine sandy) textured upper solum, with either bedrock directly below or sediment that was coarser in texture. Target locations deemed *unsuitable* for sampling, which were more common in the northern regions of the study area, usually exhibited one or more of the following criteria: (1) bedrock at the surface, (2) organic material directly overlying bedrock, (3) a high percentage of cobbles and gravels, or (4) sand, loamy sand or coarser textures in the upper profile.

At each acceptable site, the thickness of the silty mantle was determined by hand augering or by digging a small exploratory pit. Then, at the final 237 sample sites, approximately 1 kg of soil was removed either from the clean, freshly exposed loess profile provided by the exploratory pit, or obtained from the auger bucket. We retrieved one sample per site, deemed representative of the entire loess cap; loess within ≈7 cm of the underlying lithologic discontinuity was not sampled, because of likely mixing with the sediment below (Schaetzl and Luehmann, 2013). Field and lab data, not reported here, have repeatedly documented the textural uniformity in these loess deposits with depth, justifying this type of sampling method.

3.2. Lab methods

Each loess sample was gently disaggregated with a mortar and wooden pestle, after being air dried. The samples were then passed through a 2 mm sieve to eliminate gravel and large organic materials. The remaining fine earth material was sent through a sample splitter three times, to thoroughly homogenize it. Sample preparation for particle size analysis (psa) involved placing ≈1 g of soil in a 25 ml vial in which 5 ml of dispersant solution and 15 ml of distilled water were added. The dispersing solution was 35.70 g $(NaPO_3)_6$ and 7.94 g Na_2CO_3, diluted into 1 l of water (Kilmer and Alexander, 1949). Each vial with the soil sample and dispersion solution was then shaken for 2 h on a rotating table, and then run on a Malvern Mastersizer 2000 laser particle size analyzer (Malvern Instruments Ltd., Worcestershire, UK). We did not remove carbonates or organic matter from the samples, prior to psa, because the loess was not originally calcareous, and because these lower-profile samples contained almost no organic matter. Particle size data were exported into a Microsoft Excel spreadsheet in 105 size slices, or "bins," that range from 0.1 to ≈1000 μm. Using these data, detailed, continuous particle size curves can be graphed, in Excel or another graphing package (e.g., Mason and Jacobs, 1998; Hobbs et al., 2011).

3.3. Continuous textural curve filtering

3.3.1. Background and rationale

After we had graphed the particle size curves for various loess samples, it became evident that almost all of the particle size distributions were bimodal, with a large, primary peak (mode) in the silt (or very fine sand) fraction and a second, smaller peak, usually in the medium sand fraction (Fig. 4). Bimodality of loess particle size curves is not uncommon (Sun et al., 2004). Schaetzl and Luehmann (2013) observed similar particle size characteristics for loess from this area. They attributed the coarse-texture peak to mixing of sands, from below, into the silt-rich loess above, because (1) the smaller, secondary mode (in the sand fraction) peaked at particle sizes that were comparable to that of the underlying sandy glacial sediment and (2) within the loess samples, the sand mode percent volume normally became smaller nearer the surface, such that thick loess deposits were nearly unimodal and more silt-dominated. Finally, they noted that loess that directly overlies bedrock has no second (sand) mode. Post-depositional mixing processes could be expected in these thin loess deposits, and the loess particle size curves supported that supposition. Although it may be theoretically possible for some of the sand in the bimodal curves to have been transported to the sites by wind, this scenario is, in fact, highly unlikely, given the high relief and deep valleys that dominate the landscape, and the general lack of any aeolian sand landforms in the region.

Mixing of the underlying sediment, mainly sands, into the loess compromises the samples – and greatly distorts the particle size data distributions – by comparatively reducing the proportions of the original aeolian sediment. Essentially, the original characteristics of the loess particle size distribution become skewed. As a result, many loess samples that presumably were originally very silty appear much sandier because of the sand that has been mixed in from below. These kinds of "mixed sediment" loess data are common where the loess is thin (e.g., Schaetzl and Luehmann, 2013). And although these kinds of loess data are useful, we nonetheless pursued a method by which the "contaminating" sand data could be objectively removed, thereby readjusting the data to better reflect the original characteristics of the loess. We viewed this as a highly important analytical step, because accurate loess particle size data are necessary to determine source areas and transport

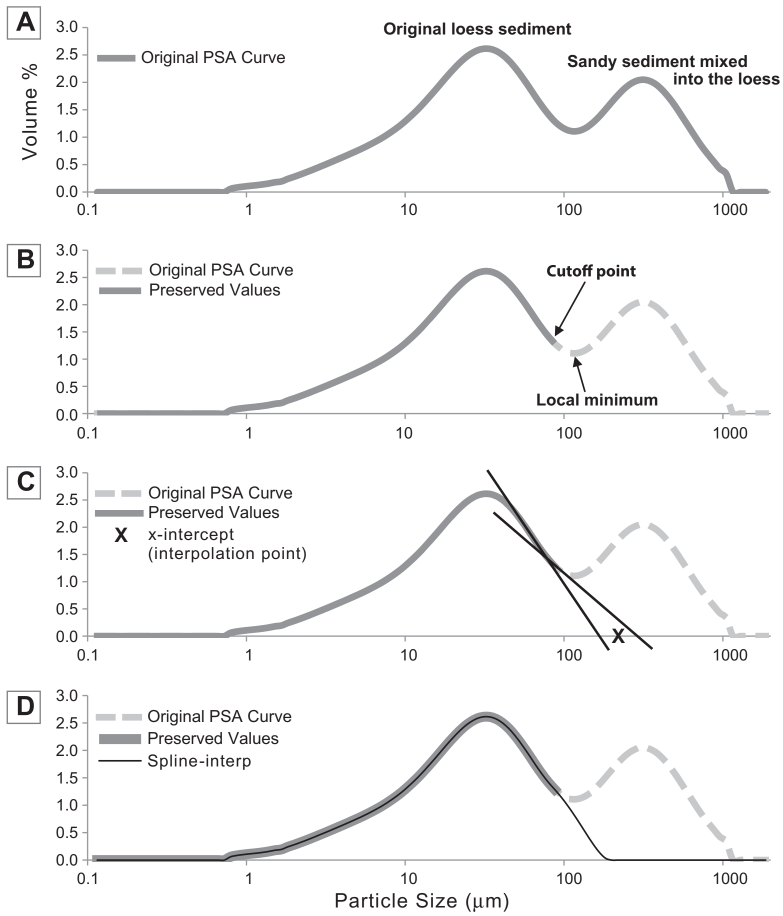

Fig. 4. Illustration of process used to filter out coarser particle size data from the (A) original bimodal distribution of particle sizes. (B) Bin values of particle sizes finer than the defined cutoff point are preserved from original particle size distribution, whereas data for bins that are coarser-textured are removed. (C) An *x*-intercept is calculated for the end-point to the interpolation, using the slope of the preserved particle size values. (D) New bin values are calculated by spline interpolation between preserved values and the *x*-intercept point. Bin values coarser than the *x*-intercept particle size value are set to zero (C).

direction (Smith, 1942; Frazee et al., 1970; Rutledge et al., 1975; Ruhe, 1984; Pye, 1995; Schaetzl and Hook, 2008).

3.3.2. Filtering the loess particle size curves: theory

In this paper, we refer to the process whereby the sand data are effectively removed from the particle size data set as "filtering." In essence, the bimodal, "mixed sediment" curve is transformed – objectively across all samples – back to its original textural characteristics, as best as possible, and in an objective and repeatable manner. The filtering algorithm used to accomplish this objective assumes that any sediment coarser than the finest particle size's expected distribution was added (later) to the original sediment, i.e., its data should be removed. Data for the coarser sediment, therefore, were filtered out by removing it, and modeling the data for some of the finer sediment, in the area of overlap. Although we cannot know the exact characteristics of the original sediment, we believe that the "filtered" data are a much better reflection of the loess' original particle size distribution than are the data from the mixed sediment, which was sampled (Fig. 4).

The filtering process consists of two parts: (1) removing the data for particle size bin values of the assumed "mixed-in" sediments and (2) interpolating new values for those particle size bins. The first step identifies which bin data should be preserved by determining the particle size bin that separates the "to-be-preserved" values from those that will be removed (Fig. 4A). We refer to the location on the *x*-axis that separates the preserved values from the removed values as the "cutoff" point (Fig. 4B). The cutoff point is the bin where the slope of the particle size distribution curve begins to reflect enrichment by the coarser sediment.

In order to interpolate a new particle size distribution curve, the range of *x*-axis values that need to be filtered (either removed completely, or changed to better reflect the original sediment's characteristics) must be determined. The lower *x*-axis value of this range is the cutoff point described above. The higher *x*-axis value of this range is the *x*-intercept interpolation point, which is the point on the *x*-axis where the "finer" particle size distribution would be expected to return to values of zero (Fig. 4C). With the range of *x*-axis values for interpolation determined, new bin values are generated between the two particle size values using a spline interpolation algorithm (Fig. 4D). Steep sloped curves can result in the interpolated curve crossing the *x*-axis before the estimated *x*-intercept. Therefore, negative interpolation values were conditionalized to zero. Finally, because the particle size bin values are expressed in volume percentages, the values of all bins are then reproportioned to sum to 100% (Fig. 5). This last operation usually forces percent silt volume data to increase. The net result is a particle size data set (curve) that better reflects the relative proportions of the various particle size fractions in the original sediment than do the original psa data.

3.3.3. Filtering the loess particle size curves: application

To accomplish these goals, a Virtual Basic macro was written for Microsoft Excel. This macro located, within the particle size distribution curve, (1) the finer particle size local maximum, in this case,

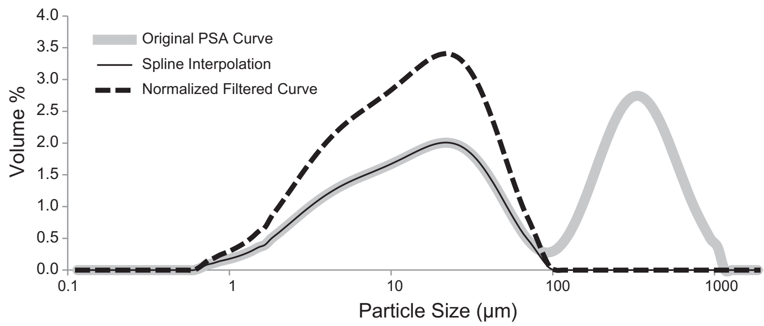

Fig. 5. An example of an original and a filtered particle size curve, illustrating how normalizing all bins to sum to 100% increases the volume percent of the preserved values.

the mode of the loess fraction, and (2) the following coarser local minimum. The macro accomplishes this task by scanning all 105 bin values, detecting shifts in value trends as it goes. During this process, the cutoff point (Fig. 4B) is identified, based on instantaneous slope values. To optimize the smoothness of the curve to be interpolated, a slope uplift threshold (UT) was also configured. This threshold limited how much the curve would be allowed to flatten, before the cutoff point would be established. The UT specified the maximum value that the new curve's slope could increase to, for particle size bins (*x*-axis) coarser than the most negative slope of the preserved bin values. Rather than set the cutoff point directly at the local minimum (Fig. 4B), the UT limited how close the slope could approach zero before the cutoff point was set. This threshold prevented preserved bin values from inducing a shoulder-like appearance in the curve that would be generated. The UT also allowed for the filtering of sand fractions that had been mixed into the original loess, but not in sufficient quantities to form a "true" second mode. In those cases where the original particle size curve had a shoulder-like appearance, the UT set the cutoff point where the curve slope began to become level. The leveling of the curve slope is the transition between the original loess sediment particle size distribution and the coarser sediment that has been mixed in. For this study, we found that an UT value of −0.003 provided consistently reasonable results. However, the UT can be adjusted to meet user needs for different curve types.

Next, the particle size value where the new, filtered curve was expected to return to zero, i.e., the *x*-intercept point, was calculated. This value would provide an end point for the forthcoming spline interpolation process. We identified two, key *x*-intercept values for characterizing the shape of the existing particle size distribution curve: (1) the *x*-intercept of the line tangent to the most negative slope of the preserved curve and (2) the *x*-intercept of the line tangent to the preserved curve at the previously described cutoff point (Fig. 4C). Ultimately, we chose to use the midpoint between these two *x*-intercepts, considering it to be the best estimate for the point on the *x*-axis where the interpolated curve should intersect with that axis. In other words, the combination of how the preserved curve's slope behaved at its (i) steepest and (ii) least steep points helped to characterize how far the interpolated curve would extend across the "new" particle size spectrum, and represented the best estimate of what the original particle size curve looked like.

Subsequently, the filtering process builds the filtered curve by first generating a copy of the preserved bins. Then, bins that will need new interpolated values are left blank, and lastly, bins expected to be zero are assigned that value. This new, limited set of bin values – with original data on the left, zeroes on the far right and blank values in the middle – essentially leaves a gap designed to be filled by the spline interpolation process. The spline function then uses the trend of the existing data to interpolate the percent volume values for the *x*-axis values that had been left blank. Because the 105 bin values are, by definition, dependent on one another and should sum to 100%, the new particle size distribution curve values must be normalized to each other by dividing individual bin values by the sum of all bin values. As a result, silt and clay values generally increased proportionately to the amount of sand that was effectively "removed" by the filtering process, i.e., the particle size curve became "higher" along parts of the particle size range that were preserved, but the relative proportions are preserved (Fig. 5). We provide the code used and instructions for processing 105 bin particle size data with that code, at the following URL (http://www.geo.msu.edu/schaetzl/links.html).

The approach described above – preserving as many observed bin values as possible and basing the shape of the modeled portion of the curve on the shape characteristics of only the preceding downslope side of the curve – avoids the errors that derive from fitted function approaches to this problem (Sun et al., 2004; Weltje and Prins, 2007). Our filtering approach also results in the preservation of as many observed bin values as possible, including the finest particle size mode and most data near it. Only particle size bins dominated by sediment that is coarser than the finest particle size distribution were modeled and recalculated.

3.3.4. Filtering the loess particle size curves: examples

Fig. 6 illustrates eight different kinds of particle size curves, in their original and their "post-filtering" forms. We chose these curves as being representative of the various sample types in the study. Note that, for samples with particle size curves which lack a second mode (Fig. 6A), the algorithm does not change the data. However, for samples that have either (1) a second mode in the sand fraction (Fig. 6D and E) or (2) some additional sand but not enough to form a "true" second mode (Fig. 6B and C), the sand data are removed and the filtering macro recalculates the data, such that a smooth curve is created. We foresee wide applications of this filtering approach to various types of mixed sediment (e.g., Mason and Jacobs, 1998; Sun et al., 2004; Tate et al., 2007; Menendez et al., 2009; Hobbs et al., 2011; Stanley and Schaetzl, 2011; Schaetzl and Luehmann, 2013).

3.4. GIS analysis

Using ArcMap 10 (ESRI, 2011) software, the filtered data were entered into a GIS attribute table. Using the geostatistical wizard module of ArcMap (ESRI, 2011), data for the various particle size data fractions were spatially interpolated using ordinary kriging, with minimum and maximum neighbors set at 12 and 15, respectively (Oliver and Webster, 1990; Hobbs et al., 2011; Scull and Schaetzl, 2011; Schaetzl and Attig, in press). Data were presented in filled contour format, and the number of isolines and their spacing were adjusted in each map in order to maximize interpretability. Separate surfaces were created for loess thickness and several loess textural variables, i.e., sand, silt, fine silt, very fine sand, etc.

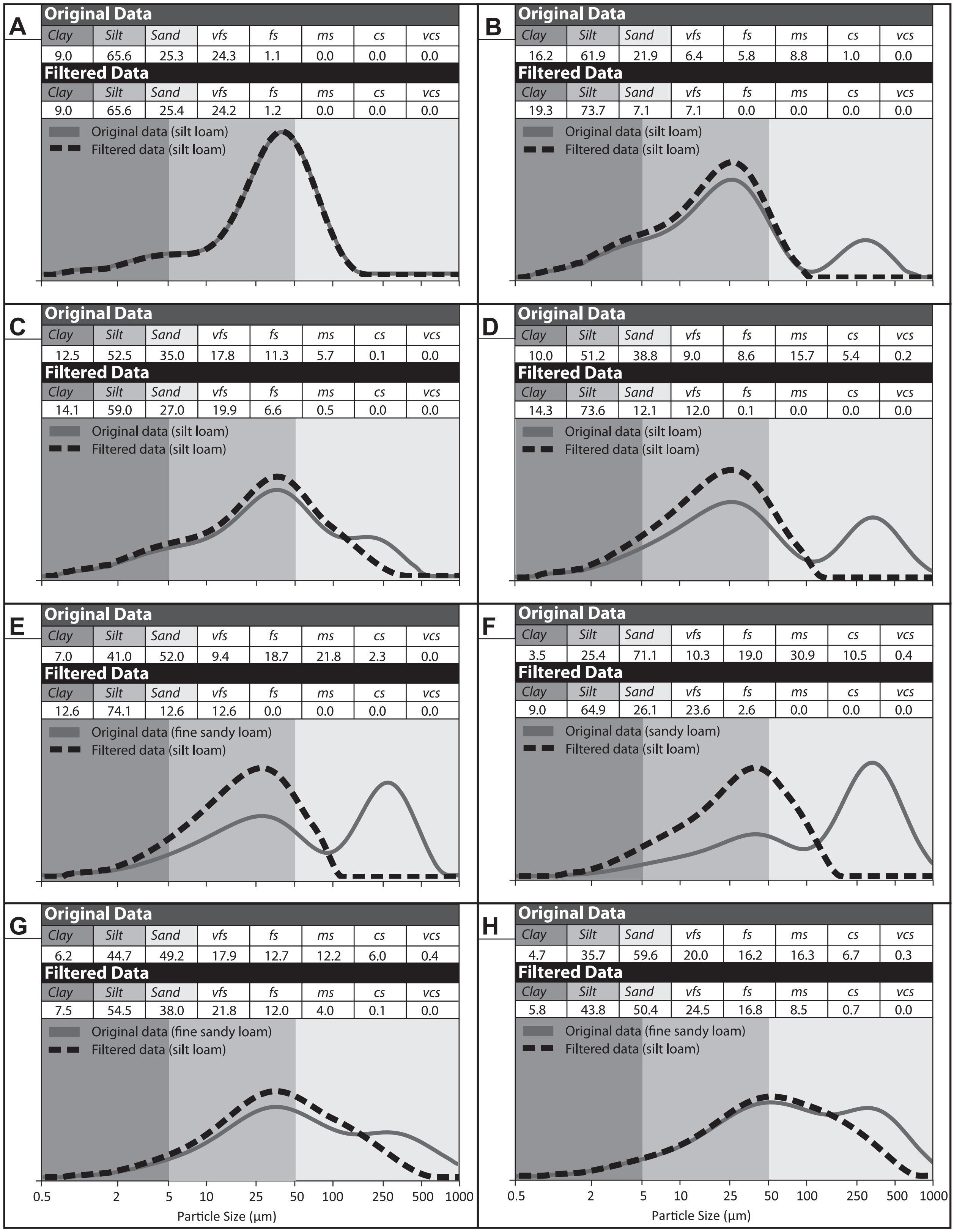

Fig. 6. The main kinds of loess particle size curves observed in the study area, in their original and their "post-filtering" forms. Associated data are also provided.

Lastly, we applied a modified version of the Trask sorting coefficient (Trask, 1932; Krumbein and Sloss, 1963) on the "filtered" particle size data, as a means of estimating the degree of aeolian sorting in the loess samples. Our modified equation is defined as the square root of the ratio of the 25% quartile value (D_{25}) to the 75% quartile value (D_{75}), for sediment between 0.01 and

1000 µm, using the 105 "bins" of filtered data from our laser particle size analyzer.

4. Results and discussion

4.1. Modeling loess distribution on glaciated landscapes

With the exception of areas of thick loess near the Mississippi and Illinois Rivers, loess in the Great Lakes region is usually thin, and exists as spatially discontinuous deposits of variable thickness and texture (Hole, 1950, 1976; Leigh and Knox, 1994; Bettis et al., 2003; Scull and Schaetzl, 2011; Jacobs et al., 2012). The most prodigious loess sources in this region were broad river valleys that carried meltwater from the Laurentide ice margin (e.g., Grimley, 2000; Jacobs et al., 2011). Nonetheless, the extent to which loess from these large, meltwater sources extends inland continues to be debated (Schaetzl, 2012; Jacobs et al., 2012). To that end, in Fig. 7 we propose that three different scenarios exist for explaining the distribution of loess on these types of landscapes. Although the model presented in Fig. 7 has potentially wide application, our discussion and examples derive from the Great Lakes region, and our study area.

Long-distance transport of loess from large meltwater valleys is depicted in Fig. 7A. In this situation, loess derived from a large meltwater river valley covers large parts of the landscape, thinning and fining with distance. Areas that lack detectable loess occur because they were geomorphically unstable during the period of deposition. Loess deposited on unstable landscapes could have been later buried by mass movements and slope failures caused by, for example, melting of buried ice or permafrost. Alternatively, the loess was eroded off sloping, possibly frozen, landscapes (Schaetzl, 2008). On the modern landscape, these areas may be typified by hummocky, high-relief, steeply sloping and/or kettled areas, commonly morainic in nature, or by deeply gullied landscapes. Additionally, in areas of thin loess, much of it may have been mixed into the underlying sediment, and hence, not easily detected. As Fig. 7A suggests, the textural and mineralogical properties of loess that exists outside of these areas would exhibit predictable spatial trends, continuing from the original source, albeit with obvious discontinuities across unstable areas (Fig. 7A).

Fig. 7B is designed to portray a loess transportation model – first proposed by Mason et al. (1999) and subsequently supported by the work of others (Schaetzl and Loope, 2008; Sweeney et al., 2005, 2007). In this example/model, loess from the meltwater valley is deposited across large parts of the landscape, somewhere within which is an active zone of transport. Commonly, the agent of transport involves active sand dunes, which remobilize the loess via saltation and enable its continued transport downwind. Because the surface of transport may also add sediment to loess that was initially deposited there, the loess downwind from it may be a mix of fine, long-distance transported loess and local-source loess that was deflated from the dunes.

Lastly, we propose that areas that lack loess could themselves be source regions – another type of geomorphically unstable area (Fig. 7A) – or landscapes of transport (Fig. 7B). That is, areas that

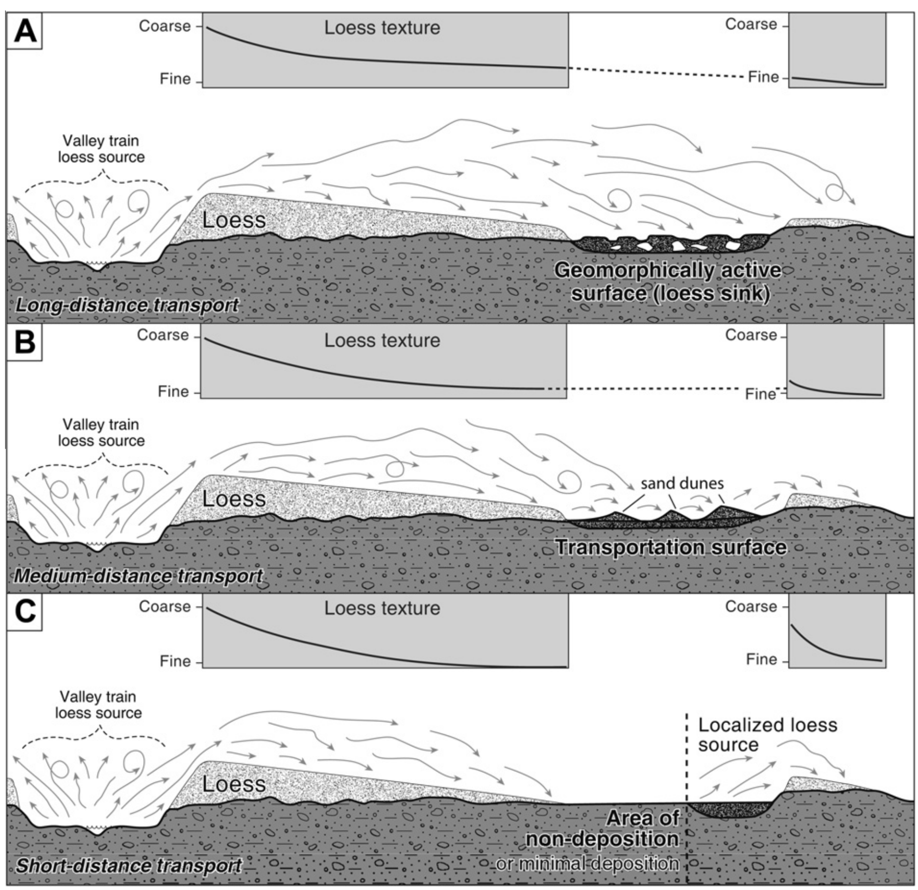

Fig. 7. Examples of traditional and non-traditional means of loess transport and deposition, as a means of explaining loess distribution on recently deglaciated landscapes. (A) A distant, valley train, loess source coupled with long-distance transport. Stable sites far from the source continue to receive loess, but that loess is undetectable in areas that are geomorphically unstable. (B) Same as "A," but in this case the loess is not transported as far. However, a surface of transport enables some of this loess to be transported beyond its normal limits. (C) Loess transport from the valley train is also spatially restricted. However, local loess sources, e.g., outwash plains or lake plains, all unrelated to the larger, valley train, source, and provide for additional loess deposition via short-distance transport. Note that the textural characteristics (and mineralogical information, if available) of the loess provide key information as to which model is most relevant.

lack loess could be the remnants of geographically isolated source areas, e.g., lake plains, outwash plains, or moraines (Schaetzl and Loope, 2008; Schaetzl and Attig, in press). Fig. 7C illustrates that these sometimes small source areas can exist far beyond the detectable "limits" of loess transport from the large river valleys, although we know of examples where they occur fairly close to these valley trains (e.g., Schaetzl, 2012). Stanley and Schaetzl (2011) identified a broad, hummocky moraine, with abundant ice-walled lake plain deposits, as an example of just such a source area for an isolated loess deposit in central Wisconsin. Loess near to these "interior" source areas could have been enriched with local, coarse-textured sediments and have rapidly changing spatial trends away from them, which may enable its differentiation from other "interior" and isolated loess deposits that are tied to longer-distance transport from large valleys.

Mineralogical differences may also provide insight into loess deposits, i.e., whether they fit into scenario A, B or C (Grimley, 2000). In scenario A, the loess should have generally similar mineralogy throughout, although we recognize that mineralogy is also a function of particle size, which will vary with distance from the source. Heavy minerals will be deposited first, because of density, whereas clay minerals will travel farther (Muhs and Bettis, 2000). Minerals concentrated in the coarser sand fractions will also be preferentially concentrated nearer the source areas. Carbonate mineralogy will also change, due to the factors mentioned above as well as differential leaching intensities associated with loess thickness and the effects of the acidic, underlying soils on thin loess, far from the source (Smith, 1942). Slight differences in mineralogy may also exist for loess deposits that occur upwind vs downwind from the surface of transport shown in scenario B, depending on how much local-source sediment was contributed by the dunes themselves, and how different their mineralogy is from that of the valley train deposits. Importantly, however, loess downwind of the local source (Fig. 7C) may have notably different mineralogy than loess from the meltwater valley, depending again on a number of local geologic factors.

We believe that our data suggest that the loess deposits in the western Upper Peninsula of Michigan formed under scenario C. Although we lack mineralogic data for this loess, it does have complex, short-range spatial variations in texture and thickness. Such patterns support the hypothesis that the loess has been deflated from small, local source areas, and which is reflective of generally short-distance transport. These patterns suggest that the loess is not a distal facies of some larger loess deposit sourced from the Mississippi Valley.

4.2. Spatial characteristics of Peshekee loess: the big picture

The loess deposits within the Peshekee loess region are thin and discontinuous – being mainly preserved on uplands. They often overlie glacial outwash, till, and/or Precambrian bedrock. As a result, virtually all the loess samples have a bimodal textural curve, due to sediment from below being mixed upward (Fig. 6; Schaetzl and Luehmann, 2013). Fortunately, the filtering method discussed and illustrated above effectively negates the effects of this post-depositional mixing, enabling us to use loess textural data that more closely approximate their original composition.

NRCS soil maps illustrate clear differences in loess thicknesses and surface texture across this region. These maps show that uplands in the southern regions of the study area have soil series with silt loam surface textures (mainly in the Goodman and Wabeno series), whereas cobbly silt loam loessal soil series (Champion, Michigamme, Petticoat, and Dishno series) are more common on uplands in the central region (Table 2; Berndt, 1988; Linsemier, 1997; Schwenner, 2007). In the northern part of the study area, Keewaydin soils are mapped; they have cobbly fine sandy loam surface textures.

More importantly, soil series with *thicker* loess caps (Petticoat, Goodman, and Michigamme series) are commonly mapped toward the south, whereas soil series with *thinner* loess caps (Wabeno, Champion, Dishno, and Keewaydin series) are mapped in the northern parts of the study area (Table 2). Thus, based solely on data from NRCS county soil surveys, it appears that the loess mantle in the Peshekee loess region gets thinner and coarser, from south to the north. Data from our research agree with NRCS soil maps; Fig. 8A shows that loess thicknesses range between ≈20 and 70 cm, and are generally thickest (>50 cm thick) in southern and southwestern Iron County, progressively thinning toward northeastern Marquette County, where loess deposits are commonly <20 cm thick, or undetectable. These data are similar to reports of loess thicknesses in the western Upper Peninsula by Scull and Schaetzl (2011) and the loess thickness data reported near the Peshekee River by Schaetzl and Liebens (1992, 1993).

Texturally, our data show that loess samples with the greatest contents of fine, medium and coarse silt (12–50 μm fraction), i.e., the siltiest ones, generally occur in eastern Iron County, near the southern margins of the study area, and extend into southwestern Marquette County (Fig. 8B). In addition, mean weighted particle size (MWPS) data (Fig. 8F) show a prominent SW–NE spatial trend; samples in the southwest have lower MWPS values (≈45 μm), whereas samples in the northeast have higher MWPS values (≈70 μm). In sum, our data are in agreement with NRCS soils data, which suggest that loess deposits progressively become thinner and coarser in texture toward the northeast.

Traditionally, loess deposits are thicker and coarser near their source and become thinner and finer-textured downwind (Smith, 1942; Frazee et al., 1970; Olson and Ruhe, 1979; Muhs and Bettis, 2000). Loess in the Peshekee region, however, exhibits very different spatial trends; it is coarsest where it is thinnest, and vice versa (Fig. 8A and F). If the dominant source area(s) for this loess is (are) in the southern parts of the study area, or beyond it to the south and west, as Fig. 8A suggests, then the MWPS of the loess should fine to the north. However, MWPS data (Fig. 8F) show that loess deposits gradually get coarser in that direction. We suggest that these seemingly contradictory spatial trends occur because of multiple and heterogeneous source areas within the study area, i.e., there are actually multiple, smaller, and overlapping loess deposits and source areas within the larger Peshekee loess region. Perhaps the best way to confirm this hypothesis is to examine its spatial characteristics at larger scales, as we do below.

4.3. Rational for multiple loess regions

As suggested in Fig. 8, the Peshekee loess region contains a variety of loess deposits of different character with regard to texture and thickness. We attempted different ways with which to represent and map these deposits, as they obviously overlap and do not have discrete boundaries. Therefore, instead of focusing on the spatial extent of each of the smaller, inset loess sheets, and defining their periphery, we instead defined their "core areas" and emphasize the characteristics of those cores.

We divided the Peshekee loess region into four core areas, each defined by, and named for, their unique loess character and for a local physical/cultural feature of prominence. From south to north, we describe the Amasa, Republic, Covington, and Champion cores (Fig. 9). The derivation and delineation of these cores was largely driven by spatial patterns of loess thickness, MWPS, and the percentage of contents within the 2–125 μm (silt plus very fine sand) fraction (Fig. 9). Below is a discussion of the spatial distribution of the loess core areas and the various characteristics that were used to differentiate one core area from another.

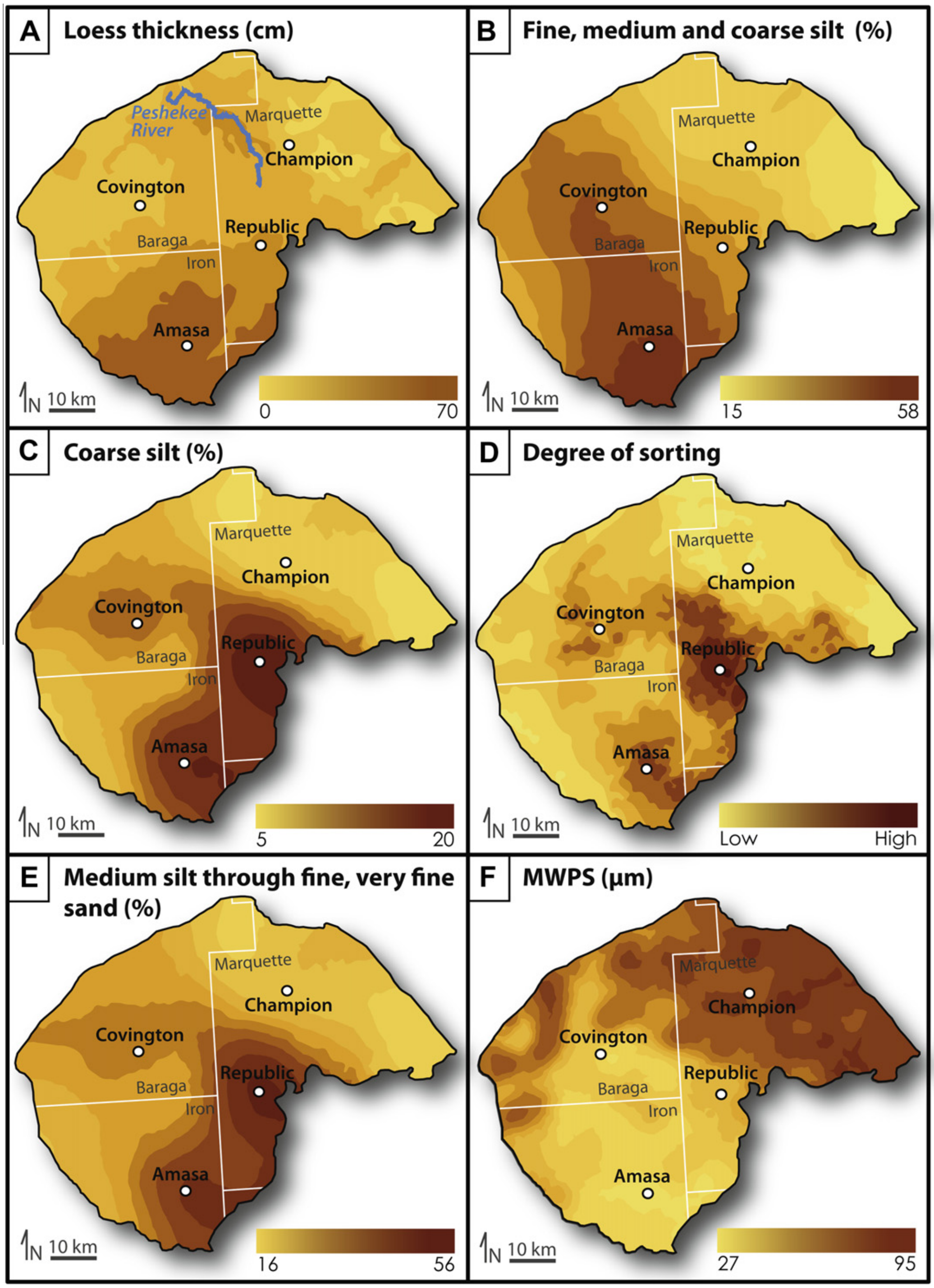

Fig. 8. Interpolated maps of different particle-size fractions, for the Peshekee loess deposits. Filled isoline values do not necessarily occur at equal intervals, as per the default mapping routine in ArcGIS. The four main loess "core" areas are also shown. (A) Loess thickness (cm). (B) Content of fine, medium and coarse silt (12–50 μm). (C) Content of coarse silt (35–50 μm). (D) Degree of sorting. (E) Content of medium silt through fine, very fine sand (25–75 μm). (F) Mean weighted particle size (μm).

4.4. Peshekee loess "core" regions

The Amasa core, located near the southern margins of the study area (Figs. 8 and 9), has some of the thickest and siltiest loess deposits in the Peshekee loess region. It represents the northernmost edge of the loess mapped by Thorp and Smith (1952) (Fig. 1). Loess deposits within the Amasa core generally have loess thicknesses >45 cm, whereas loess deposits ≈25 km directly NW, near the Covington core, are generally <30 cm thick (Table 3; Figs. 8A and 9). Particle-size curves from four loess samples within the Amasa core area illustrate that this loess usually has a modal particle-size value of ≈41 μm (coarse silt) and a moderate degree of sorting (Fig. 9; Table 3). The MWPS for these samples (39.4 μm) is much finer than the loess in the Republic and Champion cores, farther north (MWPS values of ≈55 and 70 μm, respectively) (Figs. 8F and 9). Greater loess thicknesses in the Amasa core, coupled with finer textures (Table 3), suggest that the loess deposits here are a distal part of the thicker, Iron County loess deposit,

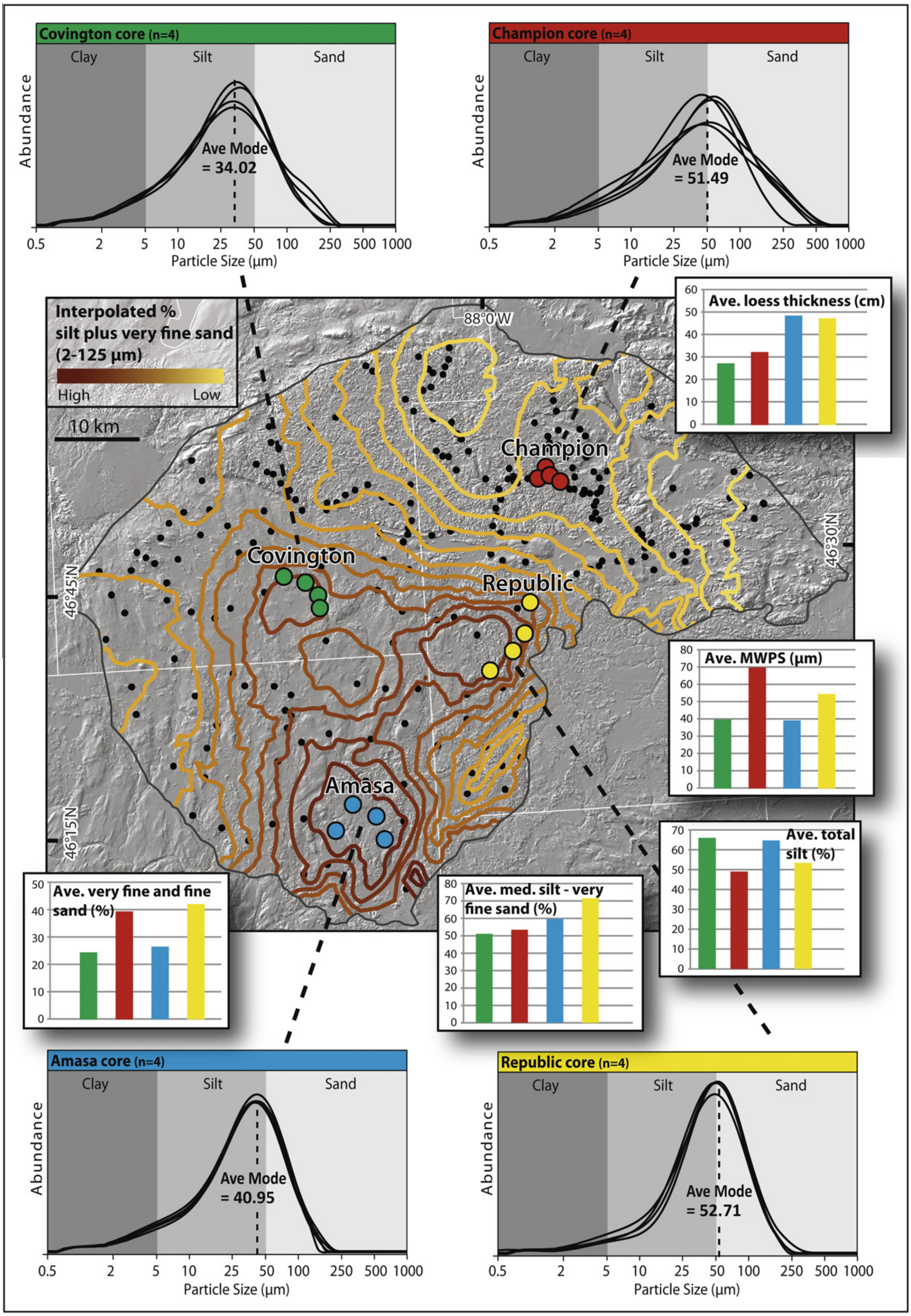

Fig. 9. Locations of the four loess core areas (each identified by four points) within the Peshekee loess region, set on a background isoline map of loess content (the 2–125 µm fraction). These data can be used to identify the differences and similarities among the four core areas. Data from these four samples were then used to create particle-size distribution curves, typical of each loess core region. In addition, mean data from these four sites are shown as histograms of loess thickness, weighted particle size, total silt (6–50 µm), medium silt through very fine sand (25–125 µm), and total very fine and fine sand (50–250 µm) for the four loess samples.

Table 3
Summary of the general characteristics of each loess core area, within the Peshekee loess region.

Loess core area	Loess thickness	Degree of sorting	% silt content	Particle-size mode
Amasa	Thick	Moderately high	Large	Moderately small
Covington	Moderate	Moderate	Large	Small
Republic	Thick	High	Moderately large	Large
Champion	Thin	Low	Small	Large

which is located primarily in Iron County, MI, but extends into Baraga and Marquette Counties, and into the bordering counties in Wisconsin (Scull and Schaetzl, 2011). Loess in the Iron County deposit (Fig. 2) is thick and silty, much like that in the Amasa core (Schaetzl and Attig, in press).

The Covington core is located mainly in southern and eastern Baraga County. Although the loess deposits in the Covington core generally are silty and moderately sorted, they nonetheless have lower amounts of the coarser size fractions, e.g., 25–75 μm, than do the loess deposits in the Amasa core, i.e., they are more "fine-silty" (Fig. 8; Table 3). Additionally, loess in the Covington core is considerably thinner than loess in the Amasa core (Figs. 8 and 9; Table 3). Mean values for four Covington core loess samples are: thickness ≈28 cm, and a particle size mode of ≈34 μm. In contrast, the Amasa core loess samples have values of 49 cm, with a mode ≈41 μm (Fig. 9).

The Republic core is located near the eastern and southeastern margins of the Peshekee loess region, in western Marquette County. Loess thicknesses within the Republic core are comparable to thicknesses mapped in the Amasa core (≈50 cm). However, textural curves from the Republic core show that loess deposits here are better sorted and much coarser, with a mean modal particle-size value of ≈53 μm; loess in the Amasa core – to the south – is much finer with a mean modal particle-size of ≈41 μm (Figs. 8 and 9; Table 3). Moreover, Republic core deposits have large amounts of medium silt through very fine sand (≈70%), whereas Amasa core deposits have about 10% less of this size fraction, and are not as well sorted (Figs. 8 and 9). Thus, the main attributes that differentiate the Republic core from the Amasa core are particle size and degree of sorting.

The northernmost loess core within the Peshekee loess region, the Champion core, is located within the Peshekee Highlands physiographic region (Schaetzl et al., 2013) which is a high relief, bedrock-dominated landscape. The other three core areas all occupy lower relief areas where glacial deposits are thicker. Bedrock outcrops and steep, bedrock-defended slopes are uncommon in these other core areas. Loess deposits in the Champion core are sandy. They have large MWPS values (≈70 μm), analogous to but even coarser than the Republic core samples (≈55 μm). However, Champion core loess deposits are much thinner and less sorted than are the loess deposits in the Republic core. Mean loess thickness for the Champion core is ≈33 cm and these deposits are poorly sorted, whereas loess in the Republic core has a mean thickness of ≈48 cm and is quite well-sorted (Figs. 8 and 9).

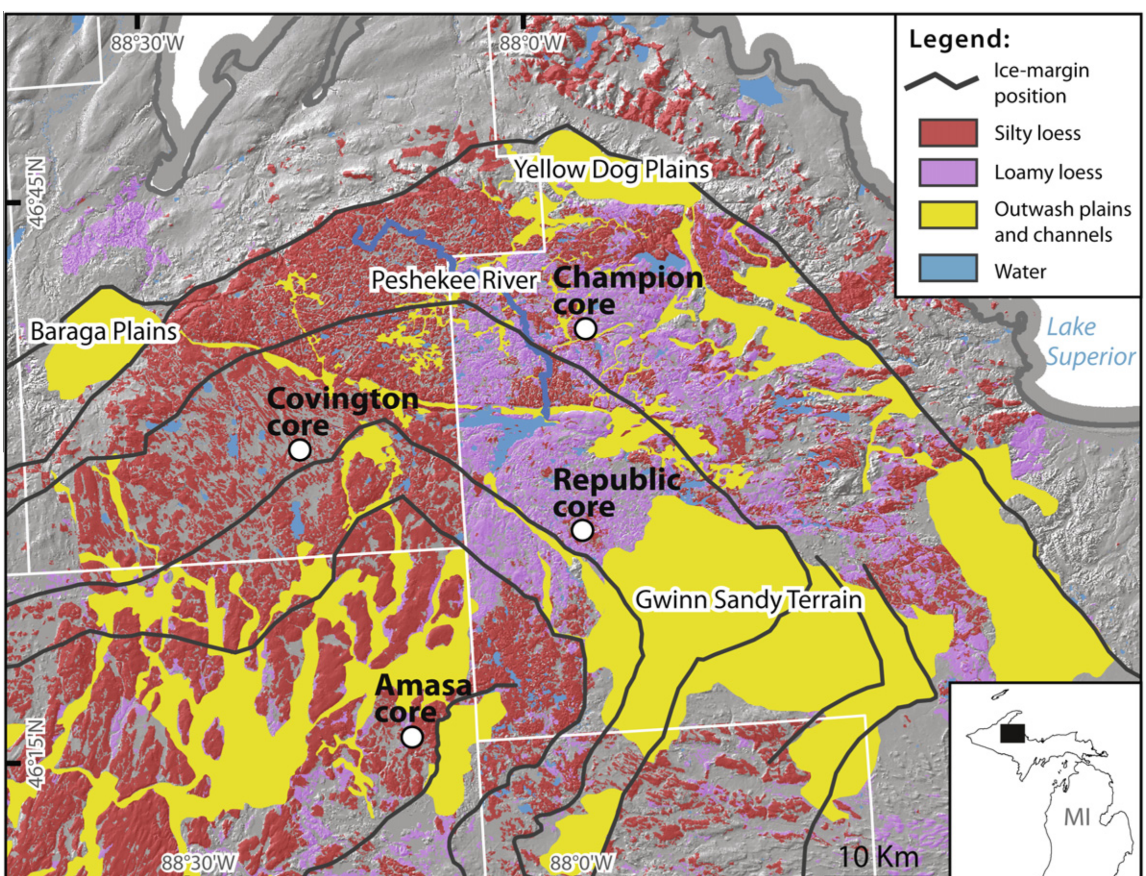

Fig. 10. Map of the potential local source areas for loess deposits within the study area. Yellow areas are outwash plains and channels, whereas red areas are soils which have formed in silty loess, as indicated on NRCS county soil surveys. (For interpretation of the references to color in this figure legend, the reader is referred to the web version of this article.)

4.5. Possible source areas

Loess is dominantly silt-sized (Pye, 1984, 1995) and thus is capable of transport in suspension for a considerable amount of time and for tens of kilometers from its source area. Sandier aeolian sediment, within 50–75 μm fraction, however, likely does not travel far from its source, giving it the potential to accumulate in large quantities at sites near to its source area. Scull and Schaetzl (2011) showed that the loess deposits in the western UP are thickest (between ≈50 and 85 cm) in southern and central Iron County, near to, but south of, the Amasa core. Schaetzl and Attig (in press) confirmed these findings and suggested that the loess in Iron County has been sourced from end moraines and small outwash sluiceways (Fig. 10), similar to loess in central Wisconsin that also lies immediately distal to a large, broad, hummocky end moraine (Stanley and Schaetzl, 2011). Schaetzl and Attig (in press) also suggested that the loess in southern Iron County was particularly thick because the high drumlins that it mantles here, in this glacial reentrant area, may have been exposed subaerially long before other, nearby, landscapes were. Moreover, loess deposits generally become finer in texture toward southern and central Iron County because these loess deposits are furthest from their dominant source area – the end moraines that surround this glacial reentrant area (Fig. 3).

Additionally, there is clear evidence that vegetation had become established in the region prior to the Marquette advance, which formed the Marquette moraine (Fig. 3) ≈11,500 cal yrs BP. At this time, advancing ice buried the Lake Gribben forest bed, near Palmer in Marquette County (Lowell et al., 1999). Thus, the uplands within Iron County and the Peshekee Highlands were probably vegetated at the time of loess deposition, which may have acted as a trap/sink for fine-grained aeolian sediment (Mason et al., 1999). Our data support the conclusions offered by Schaetzl and Attig (in press), and show loess thicknesses decreasing north from the Amasa core, as MWPS increases toward the St. Johns moraine (Figs. 3 and 8A). Loess MWPS also increases west from the Amasa core. In this area a series of broad, through-flowing outwash channels occupy the landscape (Fig. 10). These channels probably served as local loess sources. Taken collectively, these data suggest that the Amasa core, like the Iron County loess, was sourced from end moraines, broad outwash plains, and smaller, through-flowing meltwater channels (Fig. 10).

Similar to the Amasa core, loess within the Covington, Republic, and Champion cores was likely derived from local source areas (Fig. 7C). Evidence for this conclusion lies in the variable thicknesses and textures of the loess deposits – even at sites within close proximity (Fig. 8A). Extensive ice-marginal and glaciofluvial landscapes occur within the Peshekee loess region; potential, local source areas – of varying character – are prevalent (Fig. 10). Within this region, ice margins are generally associated with broad, gravel-rich moraines, generally loamy/sandy in texture, and with collapse topography due to readvances over preexisting ice (Peterson, 1986). Moreover, glacial deposits north of the Watersmeet moraine (Fig. 3) tend to contain large amounts of sandy/loamy till and lacustrine silt and clay (Peterson, 1986). During the final ice retreat, numerous meltwater channels of varying size flowed through the Peshekee landscape (Fig. 10). During low-flow events, floodplain and terrace sediments would have been exposed. Winds – katabatic and otherwise – could have deflated any fine-grain sediments from these surfaces and deposited them on adjacent stable, and probably vegetated, uplands (Hobbs, 1943; Lowell et al., 1999). Proglacial outwash plains would have also presumably been exposed to similar winds, allowing for the winnowing of fine grained sediments which later could have been deposited on nearby stable uplands.

Distributions of silt and very fine sand contents do not gradually increase or decrease across and within the Peshekee loess region; instead, there are interspersed areas of silty and sandy loess. If a single source area, e.g., some distant, meltwater river, had existed for this loess, there would presumably be a steady and progressive change in loess thickness and/or particle size characteristics across the entire region, toward and away from that source (Fig. 7A). However, this type of trend does not appear within the Peshekee loess region (Figs. 8 and 9). Rather, loess texture and thickness vary over short distances. For example, loess thickness and percent silt decrease west of the Amasa core, but eventually, as the loess thins, silt contents increase again, east of the Baraga Plains and near the Covington core (Fig. 8). The Baraga Plains is a small (≈7000 ha), sandy, outwash or glaciolacustrine plain (Barrett et al., 1995; Arbogast and Packman, 2004). When examined spatially, data in Figs. 8 and 9 show that silt and fine, very fine sand contents generally increase east of the Baraga Plains, suggesting that this outwash plain may have been a localized loess source for the Covington core. We argue that local features, like the Baraga Plains, were small but significant sources for the Peshekee loess region. As long as stable (and possibly vegetated) uplands existed in the region, to capture and retain the loess, even modest contributions of loess from these types of sources could have, over just a few decades, contributed enough aeolian sediment to produce a 20–50+ cm thick loess mantle.

We suggest that the coarse loess in the Republic core is also from a local source. Republic core loess is coarse and well sorted (Table 3). The outwash surfaces of the Gwinn Sandy Terrain, itself an extensive outwash plain located in central Marquette County (Schaetzl et al., 2013), east of the Republic core, may have been the primary source for this coarse loess (Fig. 9). The Gwinn Sandy Terrain (Fig. 10) is distal to several ice margin positions that appear to have contributed much of the coarse silt and very fine sand to the Republic core. Loess MWPS values decrease toward the south, away from these ice-margin positions and outwash surfaces (Figs. 8F, 9 and 10).

Champion core loess contains large amounts of very fine sand, which presumably did not travel far from its source area (Figs. 8 and 9). Small, interspersed, meltwater streams and outwash plains, which are common in the Peshekee Highlands, (Fig. 10) were likely the dominant sources for these loess deposits. For example the Peshekee River, which carried considerable amounts of meltwater associated with the Marquette advance, flows through the western part of the Champion core (Fig. 10). The extent of the Marquette advance is indicated by the Marquette moraine (Fig. 3) (Hughes and Merry, 1978; Farrand and Drexler, 1985; Barrett et al., 1995; Lowell et al., 1999). Loess near the river is coarser and thicker than other loess deposits within the Champion core. Nearer the ice front, strong winds would have likely been able to deflate very fine sands from the Peshekee valley and deposit them on adjacent uplands (Hobbs, 1943; Schaetzl and Liebens, 1992, 1993). Moreover, north of the Champion loess core is situated the Yellow Dog Plains (YDP), an outwash plain that is also associated with the Marquette advance (Fig. 10). The YDP likely also contributed very fine sand and coarse silts to adjacent, stable uplands within the Champion core (Fig. 10; Hughes and Merry, 1978; Farrand and Drexler, 1985). Loess MWPS values increase toward the YDP, supporting this conclusion (Fig. 8). The Peshekee River and the Yellow Dog Plains may not have been the sole source for Champion core loess, being that particles likely did not travel far from their source and relief is relatively high in this area. However, our data suggest that the small, interspersed meltwater streams and outwash landscapes that exist adjacent to and near the Champion core, similar to the Peshekee River and YDP, were likely important loess sources as well (Fig. 10).

5. Conclusions

Our study confirms that loess does exist, and is widespread but locally discontinuous, in the western UP of Michigan; we have named this area the Peshekee loess region. Our research is the first to document both the extent and textural characteristics of the thin and moderately pedoturbated loess in this region.

In this paper we first address some of the analytical challenges presented by thin loess deposits like the Peshekee loess. Thin loess is usually texturally compromised, having been mixed with sediment below. As a result, we developed and employed a data "filtering" process that objectively removes (in this case) the "contaminating" sand content, thereby adjusting the data to better reflect the original characteristics of the loess. We viewed this as an important analytical step, because accurate particle-size data are essential to proper analytics. This filtering approach may also be applied to other studies where post-depositional mixing processes are known to have occurred.

"Filtered" loess data from 237 stable, upland sites show that the Peshekee loess changes in texture and thickness across short distances, unlike thicker loess deposits that exhibit gradual and predictable variation across space. We interpret these patterns as indicative of several overlapping, smaller loess deposits of varying texture and thickness, implying that the Peshekee loess is, in essence, an amalgamation of several different, small, loess sheets. Each of these "sheets" has a core area with definable properties, but their peripheries are gradual, hard to define, and overlap with adjoining loess sheets. Glacial outwash plains, broad end moraines, and meltwater sluiceways – interspersed throughout the region and along its periphery – were the likely sources for this loess. In areas like this, where the loess deposits have multiple sources and are relatively close to their source areas, loess thickness, degree of sorting, and particle-size characteristics vary considerably, even over short distances.

Acknowledgments

We acknowledge the support of this research by the National Science Foundation, grant BCS-0422108, made to Schaetzl as PI, a scholarship made to Luehmann by the Soil Classifiers Association of Michigan, and graduate office fellowships made to Luehmann and Bigsby from the Geography Department at Michigan State University. We also appreciate the helpful comments on this research by D. Muhs, D. Lusch and A. Arbogast, and an anonymous reviewer.

References

Albert, D.A., 1995. Regional landscape ecosystems of Michigan, Minnesota, and Wisconsin: a working map and classification. USDA For. Serv. Gen. Tech. Rept. NC-178. p. 250.

Albert, D.A., Comer, P.J., 2008. Atlas of Early Michigan's Forests, Grasslands, and Wetlands. An Interpretation of the 1816–1856 General Land Office Surveys. Michigan State Univ. Press, East Lansing.

Aleinikoff, J.N., Muhs, D.R., Bettis, E.A., Johnson, W.C., Fanning, C.M., Benton, R., 2008. Isotopic evidence for the diversity of late Quaternary loess in Nebraska: glaciogenic and nonglaciogenic sources. Geol. Soc. Am. Bull. 120, 1362–1377.

Arbogast, A.F., Packman, S.C., 2004. Middle-Holocene mobilization of aeolian sand in western upper Michigan and the potential relationship with climate and fire. Holocene 14, 464–471.

Barrett, L.R., Liebens, J., Brown, D.G., Schaetzl, R.J., Zuwerink, P., Cate, T.W., Nolan, D.S., 1995. Relationships between soils and presettlement vegetation in Baraga County, Michigan. Am. Midl. Nat. 134, 264–285.

Berndt, L.R., 1988. Soil Survey of Baraga County Area, Michigan. USDA Natural Resources Conservation Service, US Govt. Printing Office, Washington, DC.

Bettis, E.A., Muhs, D.R., Roberts, H.M., Wintle, A.G., 2003. Last Glacial loess in the conterminous USA. Quatern. Sci. Rev. 22, 1907–1946.

Card, K.D., 1990. A review of the Superior Province of the Canadian Shield, a product of Archean accretion. Precambrian Res. 48, 99–156.

Comer, P.J., Albert, D.A., Wells, H.A., Hart, B.L., Raab, J.B., Price, D.L., Kashian, D.M., Corner, R.A., Schuen, D.W., 1995. Michigan's native landscape, as interpreted from the General Land Office surveys 1816–1856. Rept. to the US EPA Water Division and the Wildlife Division, MI Dept. of Natural Resources, Michigan Natural Features Inventory, Lansing. 78 pp. and digital map. <http://www.mcgi.state.mi.us/mgdl>.

Environmental Systems Research Institute (ESRI), 2011. ArcGIS Desktop: Release 10. ESRI, Redlands, CA.

Farrand, W.R., Drexler, C.W., 1985. Late Wisconsinan and Holocene history of the Lake Superior basin. In: Karrow, P.F., Calkin, P.E. (Eds.), Quaternary Evolution of the Great Lakes. Geol. Assoc. Canada Spec. Paper 30, pp. 17–32.

Fehrenbacher, J.B., Olson, K.R., Jansen, I.J., 1986. Loess thickness in Illinois. Soil Sci. 141, 423–431.

Fenneman, N.M., 1938. Physiography of Eastern United States. McGraw-Hill, New York.

Follmer, L.R., 1996. Loess studies in central United States: evolution of concepts. Eng. Geol. 45, 287–304.

Frazee, C.J., Fehrenbacher, J.B., Krumbein, W.C., 1970. Loess distribution from a source. Soil Sci. Soc. Am. J. 34, 296–301.

Grimley, D.A., 2000. Glacial and nonglacial sediment contributions to Wisconsin Episode loess in the central United States. Geol. Soc. Am. Bull. 112, 1475–1495.

Hobbs, W.H., 1943. The glacial anticyclone and the continental glaciers of North America. Proc. Am. Philos. Soc. 86, 368–402.

Hobbs, T., Schaetzl, R.J., Luehmann, M.D., 2011. Evidence for periodic, Holocene loess deposition in kettles in a sandy interlobate landscape, Michigan, USA. Aeol. Res. 3, 215–228.

Hole, F.D., 1950 (reprinted, 1968). Aeolian sand and silt deposits of Wisconsin. Wisconsin Geological and Natural History Survey Map, Madison, WI.

Hole, F.D., 1976. Soils of Wisconsin. Univ. of Wis. Press, Madison, p. 223.

Hughes, J.D., Merry, W.J., 1978. Marquette buried forest 9,850 years old. In: American Association for the Advancement of Science, National Meeting.

Jacobs, P.M., Mason, J.A., Hanson, P.R., 2011. Mississippi Valley regional source of loess on the southern Green Bay Lobe land surface, Wisconsin. Quatern. Int. 75, 574–583.

Jacobs, P.M., Mason, J.A., Hanson, P.R., 2012. Mississippi Valley regional source of loess on the Southern Green Bay Lobe land surface, Wisconsin – response to comments by Randall Schaetzl, pages 574–583. Quatern. Res. 78, 152–153 (letter to the Editor).

Kilmer, V.J., Alexander, L.T., 1949. Methods of making mechanical analysis of soils. Soil Sci. 68, 15–24.

Krumbein, W.C., Sloss, L.L., 1963. Stratigraphy and Sedimentation. W.H. Freeman and Co., San Francisco, 660 pp..

Leigh, D.L., 1994. Roxana silt of the Upper Mississippi Valley: lithology, source, and paleoenvironment. Geol. Soc. Am. Bull. 106, 430–442.

Leigh, D.L., Knox, J.C., 1994. Loess of the upper Mississippi Valley driftless area. Quatern. Res. 42, 30–40.

Linsemier, L.H., 1997. Soil Survey of Marquette County Area, Michigan. USDA Natural Resources Conservation Service, US Govt. Printing Office, Washington, DC.

Lowell, T.V., Larson, G.J., Hughes, J.D., Denton, G.H., 1999. Age verification of the Lake Gribben forest bed and the Younger Dryas Advance of the Laurentide Ice Sheet. Can. J. Earth Sci. 36, 383–393.

Mason, J.A., Nater, E.A., Zanner, C.W., Bell, J.C., 1999. A new model of topographic effects on the distribution of loess. Geomorphology 28, 223–236.

Mason, J.A., Jacobs, P.M., 1998. Chemical and particle-size evidence for addition of fine dust to soils of the midwestern United States. Geology 26, 1135–1138.

Menendez, I., Cabrera, L., Sanchez-Perez, I., Mangas, J., Alonsol, I., 2009. Characterisation of two fluvio-lacustrine loessoid deposits on the island of Gran Canaria, Canary Islands. Quatern. Int. 196, 36–43.

Muhs, D.R., Aleinikoff, J.N., Stafford Jr., T.W., Kihl, R., Been, J., Mahan, S.A., Cowherd, C., 1999. Late Quaternary loess in northeastern Colorado: Part I – age and paleoclimatic significance. Geol. Soc. Am. Bull. 111, 1861–1875.

Muhs, D.R., Bettis, E.A., 2000. Geochemical variations in Peoria Loess of western Iowa indicate paleowinds of midcontinental North America during last glaciations. Quatern. Res. 53, 49–61.

Muhs, D.R., Bettis, E.A., 2003. Quaternary loess-paleosol sequences as examples of climate-driven sedimentary extremes. In: Chan, M.A., Archer, A.W. (Eds.), Extreme Depositional Environments: Mega End Members in Geologic Time. Geol. Soc. Am. Spec. Pap. 370, 53–74.

Muhs, D.R., Bettis, E.A., Aleinikoff, J., McGeehin, J.P., Beann, J., Skipp, G., Marshall, B.D., Roberts, H.M., Johnson, W.C., Benton, R., 2008. Origin and paleoclimatic significance of late Quaternary loess in Nebraska: evidence from stratigraphy, chronology, sedimentology, and geochemistry. Geol. Soc. Am. Bull. 120, 1378–1407.

Oliver, M.A., Webster, R., 1990. Kriging: a method of interpolation for geographical information systems. Int. J. Geogr. Inf. Sci. 4, 313–332.

Olson, C.G., Ruhe, R.V., 1979. Loess dispersion model, southwest Indiana, USA. Acta Geol. Acad. Sci. Hung. Tomus 22, 205–227.

Peterson, W.L., 1986. Late Wisconsinan glacial history of northeastern Wisconsin and western upper Michigan. U.S. Geol. Surv. Bull. 1652, 14.

Pregitzer, K.S., Reed, D.D., Bornhorst, T.J., Foster, D.R., Mroz, G.D., Mclachlan, J.S., Laks, P.E., Stokke, D.D., Martin, P.E., Brown, S.E., 2000. A buried spruce forest provides evidence at the stand and landscape scale for the effects of environment on vegetation at the Pleistocene/Holocene boundary. J. Ecol. 88, 45–53.

Pye, K., 1984. Loess. Prog. Phys. Geogr. 8, 176–217.

Pye, K., 1995. The nature, origin and accumulation of loess. Quatern. Sci. Rev. 14, 653–667.

Roberts, H.M., Muhs, D.R., Wintle, A.G., Duller, G.A.T., Bettis, E.A., 2003. Unprecedented last-glacial mass accumulation rates determined by luminescence dating of loess from western Nebraska. Quatern. Res. 59, 411–419.

Ruhe, R.V., 1984. Loess derived soils, Mississippi valley region: I. Soil sedimentation system. Soil Sci. Soc. Am. J. 48, 859–867.

Rutledge, E.M., Guccione, M.J., Markewich, H.W., Wysocki, D.A., Ward, L.B., 1996. Loess stratigraphy of the Lower Mississippi Valley. Eng. Geol. 45, 167–183.

Rutledge, E.M., Holowaychuk, N., Hall, G.F., Wilding, L.P., 1975. Loess in Ohio in relation to several possible source areas: I. Physical and chemical properties. Soil Sci. Soc. Am. Proc. 39, 1125–1132.

Schaetzl, R.J., Liebens, J., 1992. Spatial analysis of eolian sediments in the Peshekee Highlands, Marquette and Baraga Counties, Michigan. Presented at the Annual Meeting of the Michigan Academy of Science, Arts and Letters, Mount Pleasant, MI.

Schaetzl, R.J., Liebens, J., 1993. A possible eolian deposit in Michigan's Upper Peninsula. Presented at the 3rd International Association of Geomorphologists Conference, Hamilton, Ontario, Canada.

Schaetzl, R.J., 2008. The distribution of silty soils in the Grayling Fingers region of Michigan: evidence for loess deposition onto frozen ground. Geomorphology 102, 287–296.

Schaetzl, R.J., Hook, J., 2008. Evidence for loess in Northwest Lower Michigan: characterizing the silty mantle on the Buckley Flats Outwash Plain. Phys. Geogr. 29, 140–157.

Schaetzl, R.J., Loope, W.L., 2008. Evidence for an eolian origin for the silt-enriched soil mantles on the glaciated uplands of eastern Upper Michigan, USA. Geomorphology 100, 285–295.

Schaetzl, R.J., 2012. Comment on: Mississippi Valley regional source of loess on the southern Green Bay Lobe land surface, Wisconsin (Quat. Res. 75 (3), 574–583, 2011). Quatern. Res. 78, 149–151.

Schaetzl, R.J., Luehmann, M.D., 2013. Coarse-textured basal zones in thin loess deposits: products of sediment mixing and/or paleoenvironmental change? Geoderma 192, 277–285.

Schaetzl, R.J., Enander, H., Luehmann, M.D., Lusch, D.P., Fish, C., Bigsby, M., Steigmeyer, M., Powers, J., Forgacs, C., Pollyea, A., 2013. Mapping the physiography of Michigan with GIS. Phys. Geogr. 34.

Schaetzl, R.J., Attig, J.W., in press. The loess cover of northeastern Wisconsin. Quatern. Res. 79.

Schwenner, C., 2007. Soil Survey of Marquette County Area, Michigan. USDA Natural Resources Conservation Service, US Govt. Printing Office, Washington, DC.

Scull, P., Schaetzl, R.J., 2011. Using PCA to characterize and differentiate loess deposits in Wisconsin and Upper Michigan, USA. Geomorphology 127, 143–155.

Smalley, I.J. (Ed)., 1975. Loess: lithology and genesis. Benchmark Papers in Geology no. 26. Dowden Hutchinson and Ross, Stroudsburg, PA, p. 448.

Smith, G.D., 1942. Illinois loess: variations in its properties and distribution. Univ. Ill. Agric. Exp. Stat. Bull. 490.

Stanley, K.E., Schaetzl, R.J., 2011. Characteristics and paleoenvironmental significance of a thin, dual-sourced loess sheet, north-central Wisconsin. Aeol. Res. 2, 241–251.

Sweeney, M.R., Busacca, A.J., Gaylord, D.R., 2005. Topographic and climatic influences on accelerated loess accumulation since the last glacial maximum in the Palouse, Pacific Northwest, USA. Quatern. Res. 63, 261–273.

Sweeney, M.R., Gaylord, D.R., Busacca, A.J., 2007. Evolution of Eureka Flat: a dust-producing engine of the Palouse loess, USA. Quatern. Int. 162–163, 76–96.

Sun, J.M., 2002. Provenance of loess material and formation of loess deposits on the Chinese Loess Plateau. Earth Planet. Sci. Lett. 203, 845–859.

Sun, D., Bloemendal, J., Rea, D.K., Zhisheng, A., Vandenberghe, J., Huayu, L., Ruixia, S., Tungsheng, L., 2004. Bimodal grain-size distribution of Chinese loess, and its palaeoclimatic implications. Catena 55, 325–340.

Tate, S.E., Greene, R.S.B., Scott, K.M., McQueen, K.G., 2007. Recognition and characterisation of the aeolian component in soils in the Girilambone Region, north western New South Wales, Australia. Catena 69, 122–133.

Thorp, J., Smith, H.T.U., 1952. Pleistocene eolian deposits of the United States, Alaska, and parts of Canada. National Research Council Committee for the Study of Eolian Deposits, Geological Society of America, Scale 1:2,500,000.

Trask, P.D., 1932. Origin and Environment of Source Sediments of Petroleum: Houston, Gulf Publishing Co.

Wascher, H.L., Humbert, R.P., Cady, J.G., 1947. Loess in the southern Mississippi valley: identification and distribution of loess sheets. Soil Sci. Soc. Am. J. 12, 389–399.

Weltje, G.J., Prins, M.A., 2007. Genetically meaningful decomposition of grain-size distributions. Sediment. Geol. 202, 409–424.